Bioactive Materials 25 (2023) 307–318

Contents lists available at ScienceDirect

Bioactive Materials

journal homepage: www.keaipublishing.com/en/journals/bioactive-materials

Regulating macrophage-MSC interaction to optimize BMP-2-induced osteogenesis in the local microenvironment

Fei Jiang [a,b,c,d,1], Xuanyu Qi [a,b,1], Xiaolin Wu [a,b], Sihan Lin [a,b], Junfeng Shi [a,b], Wenjie Zhang [a,b], Xinquan Jiang [a,b,*]

[a] Department of Prosthodontics, Shanghai Ninth People's Hospital, Shanghai Jiao Tong University School of Medicine, No.639, Zhizaoju Road, Shanghai, 200011, China
[b] College of Stomatology, Shanghai Jiao Tong University, National Center for Stomatology, National Clinical Research Center for Oral Diseases, Shanghai Key Laboratory of Stomatology, Shanghai Engineering Research Center of Advanced Dental Technology and Materials, No.639, Zhizaoju Road, Shanghai, 200011, China
[c] Jiangsu Key Laboratory of Oral Diseases, Jiangsu Province Engineering Research Center of Stomatological Translational Medicine, Nanjing Medical University, No. 140, Han Zhong Road, Nanjing, 210029, China
[d] Department of General Dentistry, Affiliated Hospital of Stomatology, Nanjing Medical University, No. 136, Han Zhong Road, Nanjing, 210029, China

ARTICLE INFO

Keywords:
BMP-2
Osteogenesis
IL-1β
IL-1Ra
Macrophage-MSC interaction

ABSTRACT

Bone morphogenetic protein (BMP-2) has been approved by the FDA to promote bone regeneration, but uncertain osteogenic effect and dose-dependent side effects may occur. Osteoimmunomodulation plays an important role in growth factor-based osteogenesis. Here, we explored how proinflammatory signals affect the dose-dependent osteogenic potential of BMP-2. We observed that the expression level of local IL-1β did not increase with the dose of BMP-2 in the mouse osteogenesis model. A low dose of BMP-2 could not promote new bone formation, but trigger the release of IL-1β from M1 macrophages. As the dose of BMP-2 increased, the IL-1β expression and M1 infiltration in local microenvironment were inhibited by IL-1Ra from MSCs under osteogenic differentiation induced by BMP-2, and new bone tissues formed, even excessively. Anti-inflammatory drugs (Dexamethasone, Dex) promoted osteogenesis via inhibiting M1 polarization and enhancing BMP-2-induced MSC osteo-differentiation. Thus, we suggest that the osteogenic effect of BMP-2 involves macrophage-MSC interaction that is dependent on BMP-2 dose and based on IL-1R1 ligands, including IL-1β and IL-1Ra. The dose of BMP-2 could be reduced by introducing immunoregulatory strategies.

1. Introduction

Bone morphogenetic protein-2 (BMP-2) was first approved by Food and Drug Administration (FDA) in United States in 2002 for clinical application with the dosage of 1.5mg/ml [1–3]. The FDA-approved BMP-2 dosage, determined through nonhuman primate experiments [4], has shown to effectively promote fracture healing [5,6]. However, independent assessments of the original industry-sponsored publications and independent assessment of original FDA data revealed that BMP-2-associated complications were not nominal and infrequent [4]. Some studies report that this dose even cannot achieve satisfactory osteogenic effects in repairing bone defects [7,8], and may bring with many adverse events, such as excessive osteogenesis [9], ectopic bone formation [10], inflammatory complications [11], osteolysis [12], bone cyst formation [13]. Thus, it is critical to clarify the mechanisms underlying BMP-2-induced osteogenesis and side effects.

BMP-2 induces osteogenesis relying on the activation of local bone-forming cells [14,15], especially osteoblasts and MSCs that have been intensely investigated [16,17]. In addition, their abilities in promoting osteogenesis are sensitive to BMP-2 dose, whereas 50 ng/ml or 100 ng/ml BMP-2 just induces MSCs proliferation and osteoblastic differentiation *in vitro* [18,19]. Why does the FDA use "mg/ml" to standardize the dose of commercial BMP-2 products, which may be high enough to easily cause side effects, including excessive osteogenesis? We speculate that the osteogenic potential of BMP-2 *in vivo* may be discounted by other antagonistic factors. Thus, the dose of BMP-2 must be set at a high

Peer review under responsibility of KeAi Communications Co., Ltd.
* Corresponding author. Department of Prosthodontics, Shanghai Ninth People's Hospital, Shanghai Jiao Tong University School of Medicine, No.639, Zhizaoju Road, Shanghai, 200011, China.
E-mail address: xinquanj@aliyun.com (X. Jiang).
[1] The authors contributed equally to this work.

https://doi.org/10.1016/j.bioactmat.2023.02.001
Received 5 November 2022; Received in revised form 1 February 2023; Accepted 1 February 2023
2452-199X/© 2023 The Authors. Publishing services by Elsevier B.V. on behalf of KeAi Communications Co. Ltd. This is an open access article under the CC BY-NC-ND license (http://creativecommons.org/licenses/by-nc-nd/4.0/).

level. In fact, the connective tissues protect against a broad range of pathogens (including exogenous growth factors) via orchestrating both innate and adaptive immune responses [20].

When exogenous pathogens invade the host, the innate immune system props up the first defense [21,22], meanwhile releasing inflammation-related factors that may interfere with the function of bone-forming cells [23,24]. As a consequence, osteogenesis is inhibited. However, exogenous BMP-2 can activate macrophages in the bone-repairing microenvironment [25]. Macrophages are classified into M1 and M2 subtypes, according to their functional properties, surface markers, and inducers [26]. M1 macrophages secrete an array of pro-inflammatory cytokines, such as TNF-α, IL-6 and IL-1β [27,28]. Interleukin-1 (IL-1β) and IL-1R1 are leading mediators between innate immunity and inflammation in all cells and organs [29,30]. Julier Z et al. have found that BMP-2 can stimulate M1 macrophages to release IL-1β that bind to the IL-1R1 on the surface of bone-forming cells (MSCs and osteoblasts), thereby inhibiting osteogenic differentiation and subsequent bone regeneration [31]. In contrast, another study has reported that BMP-2 scaffolds can induce M2 macrophages to promote bone regeneration [32]. Wei F et al. reported the immunoregulatory role of BMP-2 on macrophages and the subsequent effects on osteogenesis seemed to be complex. They found gelatin sponge incorporated with 20 μg/mL BMP-2 rendered significantly enhanced M1 infiltration, but the supplementation of BMP-2 dramatically diminished the expression of M1 markers, including IL-1β, IL-6, and iNOS [33]. Therefore, we hypothesized that BMP-2 exerts dose-dependent effects on osteogenesis and side effects through regulating macrophage-MSC interaction in the local microenvironment.

In this study, we profiled macrophage-MSC interaction at different BMP-2 doses to elucidate the mechanism of BMP-2-induced osteogenesis. Our findings may provide theoretical evidence for repairing bones with a lower BMP-2 dose in clinical practice.

2. Materials and methods

2.1. Study design

All *in vitro* experiments were replicated for at least three times independently. Appropriate statistical methods were used to analyze the data of experiments. For *in vivo* studies, mice were randomized into experiment groups. All surgical procedures and sample analyses adhered to the principles of blindness and uniformity. The *n* value of each experiment is shown in the figure legends. Statistical methods are described in the "Statistical analysis" section.

2.2. Mice

Wild-type C57BL/6 mice were provided by the Animal Laboratory Center of Shanghai Ninth People's Hospital Affiliated with Shanghai Jiao Tong University. C57BL/6-IL-1β$^{em1(Luc\text{-}eGFP)Smoc}$ mice were purchased from Shanghai Model Organisms Center, Inc. The experimental protocols were approved by the Animal Experimental Ethical Committee of Shanghai Ninth People's Hospital Affiliated with Shanghai Jiao Tong University.

2.3. Bio-materials preparation

The CPC (calcium phosphate cement) particles and *Escherichia coli*-derived rhBMP-2 (recombinant human BMP-2, carrier-free, >95% purity) were purchased from REBONE Biomaterials Company (Shanghai, China). The size of the CPC particles was set at 5 mm in diameter and 5 mm in height. Silk sponges used in this work were the same as those used in previously reported studies [34] and prepared into a 5–6% (w/v) silk solution. Porous structures of silk sponges were prepared by lyophilization and then autoclaved at 121 °C for 20 min. The silk sponges were finally trimmed to 5 mm in diameter and about 3 mm in height. The CPC particles and silk sponges were fumigated by ethylene oxide vapor in advance. The BMP-2 was dissolved in sterile PBS, with adequate mixing ensured. The BMP-2 solution (0.05 mg/ml, 0.30 mg/ml and 1.50 mg/ml [w/v]) was distributed on two kinds of scaffolds in sterile conditions, till being completely absorbed by the scaffolds.

2.4. In vitro release of BMP-2 from CPC particles and silk sponges

To measure the release of BMP-2 from CPC particles and silk sponges *in vitro*, the BMP-2/CPC particles and BMP-2/silk sponges were respectively put into the vials containing 1 ml PBS solution. The vials were incubated at 37 °C for 7 d. At each time point, the release medium was collected and replaced with an equal amount of fresh PBS. The amount of released BMP-2 was measured using a BMP-2 ELISA kit (BGK8C060, PeproTech, USA). The release profile was defined as the cumulative percentage of released BMP-2 (%, w/w) during the period of incubation. The results were shown in Supplementary Fig. 5.

2.5. Animal experiments

The 8-week-old mice (the weight of mice was about 20 g) were selected for our study according to published references on bone regeneration [35–37]. They were anesthetized with isoflurane for operations of femoral defect model and dorsal subcutaneous transplantation. To create a model of femoral defect, the limb to be operated was shaved and a lateral approach to the femur was performed without damaging the muscle. The periosteum was lifted and the bone defect was made in the mouse femur using a 1 mm bone drill. To prepared for dorsal subcutaneous transplantation, a longitudinal incision was performed on the mice prepared dorsal parts to separate the subcutaneous tissue. BMP-2/CPC particles or BMP-2 sponges were implanted subcutaneously through the incision, which was then sutured. The mice were euthanized at the scheduled time point after surgery, and the subcutaneous samples were subjected to histological analysis, flow cytometry and micro–computed tomography (micro-CT). In 0.05 mg/ml + Dex group, 200 μl Dex solution (5 μg/ml) was injected around the 0.05 mg/ml BMP-2/CPC particles at 2 h after transplantation. The Dex injection was performed once a day during the first 3 days for 0.05 mg/ml + Dex group. The IL-1β neutralizing antibody was injected around 0.05 mg/ml CPC particles after transplantation. The neutralizing antibody against IL-1β 300 μg per mouse (I-437, Leinco Technologies; USA) were injected intraperitoneally on the day before subcutaneous transplantation. The Armenian hamster IgG isotype (I-140, Leinco Technologies; USA) were used as control. There were six mice in each experimental group.

2.6. Micro-CT scanning of BMP-2/CPC samples

Samples were fixed by 10% formalin and scanned with a micro-CT 50 (Scanco Medical AG) in a holder (diameter 34 mm and height 110 mm) at 70 kV peak (kVp), 200 μA, 14 W. A voxel size of 20 μm and an integration time of 300 ms were adopted. Scans were reconstructed with a nominal isotropic resolution of 35 μm. After scanning, all images were submitted to three-dimensional (3D) reconstruction. Bone and CPC particles were marked by yellow and red, respectively. Their intensity values were calculated using the scanner software (IPL, Scanco Medical AG) to show the osteogenic effects. The threshold of bone intensity was between 180 and 300, while that of CPC particles was 570–800.

2.7. Histological analysis of 14-d BMP-2/CPC samples

After micro-CT scanning, the subcutaneous samples in the 14-d group were embedded in polymethylmethacrylate (PMMA) and cut into sections 150 μm thick using a microtome (Leica, Germany). These sections were gradually ground and polished to 40 μm in thickness for observation of osteogenesis around BMP-2/CPC particles.

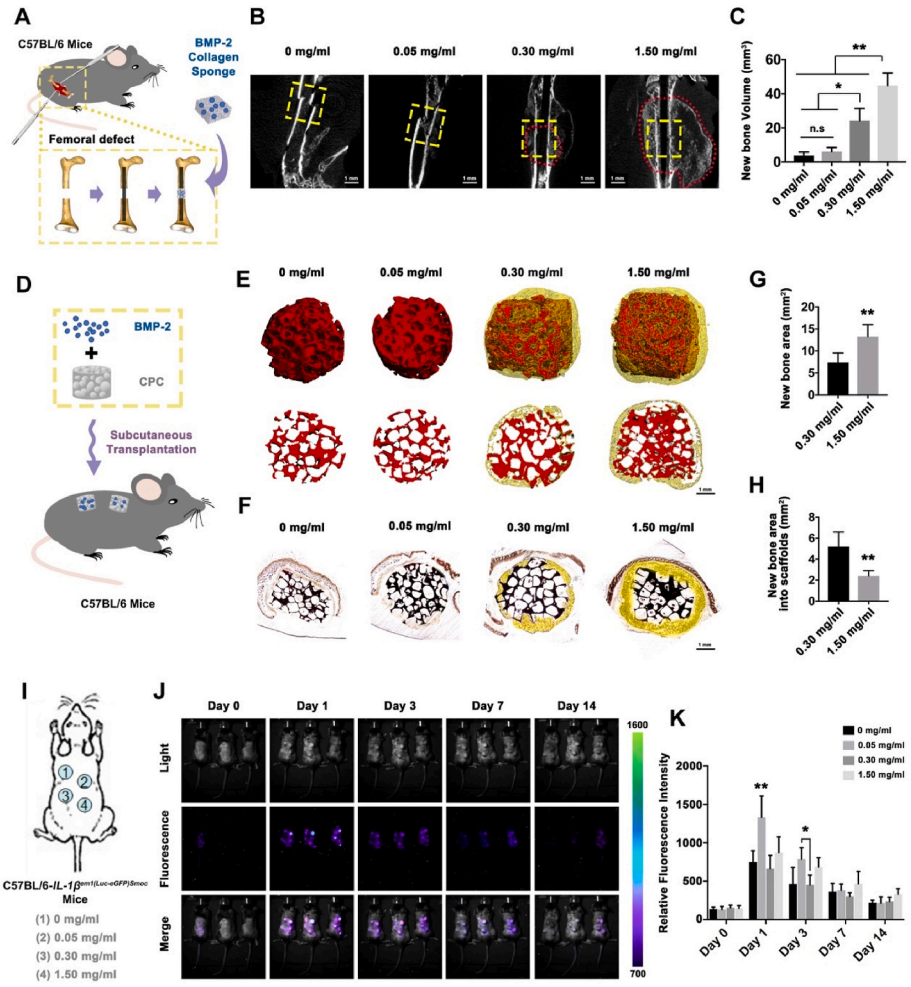

Fig. 1. Local osteogenesis and IL-1β activity induced by different BMP-2 doses. [A] Schematic diagram of the femoral defects in mice repaired by BMP-2/collagen sponges. [B] Fourteen days after operation, bone regeneration was detected by micro-CT. The defects were marked by yellow squares and new bone by red dotted lines. Scale bar: 1 mm [C] The new bone volume was measured and analyzed by one-way ANOVA. [D] Schematic diagram of CPC particles subcutaneously implanted in mice. [E] Fourteen days after operation, bone regeneration was measured by micro-CT and [F] PMMA-embedded sections. New bone (marked as yellow) formed in and around porous scaffolds (marked as red or black). Scale bar: 1 mm [G] Total percentage of new bone area in the BMP-2/CPC sections. [H] The percentage of new bone area in the CPC particles to total new bone area. [I] Schematic diagram of BMP-2/CPC particles transplanted in C57BL/6-IL-1β$^{em1(Luc\text{-}eGFP)Smoc}$ mice. [J] Representative fluorescence images of C57BL/6-IL-1β$^{em1(Luc\text{-}eGFP)Smoc}$ mice at 0, 1, 3, 7,14 d after transplanting different doses of BMP-2/CPC particles. [K] Fluorescence intensity was quantified by statistical analysis at 0, 1, 3, 7,14 d after transplantation.

2.8. Local IL-1β promoter activity after subcutaneous transplantation of BMP-2/CPC particles

The 8-week-old C57BL/6 mice (about 20 g weight) carrying *IL-1β*, a promoter-driven firefly luciferase reporter gene, were used. There were six replicates of C57BL/6-IL-1β$^{em1(Luc\text{-}eGFP)Smoc}$ mice in each group. Four different BMP-2/CPC particles (0 mg/ml, 0.05 mg/ml, 0.30 mg/ml, 1.50 mg/ml) were transplanted into the dorsal parts of the transgenic mice. D-Luciferin potassium salt (0.1 mM, Wako Pure Chemical Industries, Japan) was dissolved in distilled water. The solution was kept at room temperature. At 1, 3, 7 and 14 d after transplantation, the D-luciferin solution was injected intraperitoneally into the transgenic mice anesthetized through isoflurane inhalation. The peak of D-luciferin bioluminescence signal lasted around 15 min. D-Luciferin was detected using a fluorescence detector (excitation λ = 330 nm, emission λ = 530 nm) as previously reported [38,39]. The images of D-luciferin bioluminescence signal are shown in Fig. 1J.

2.9. Macrophage-MSC interaction in 3-d subcutaneous BMP-2/CPC samples

Based on the results of subcutaneous IL-1β promoter activity, we investigated the IL-1β expression, M1 macrophage infiltration and Osx-positive osteoblast distribution in 3-d samples. The samples of subcutaneous BMP-2/CPC particles in the 3-d group were fixed by 10% formalin, decalcified, embedded in paraffin and sectioned (4 mm thickness). Immunohistochemistry was used to detect the expression of IL-1β, iNOS and Osx in the sections. The sections were deparaffinized by xylene, hydrated with gradient ethanol, and subjected to heat-mediated antigen retrieval in citrate buffer at pH 6.0. The samples were then blocked by 5% sheep serum for 30 min and incubated separately with primary antibodies overnight at 4 °C. Thereafter, the samples were washed 3 times with PBS for 5 min per time and HRP-conjugated with secondary antibodies (MXB Biotechnologies, China) at room temperature for 20 min. Finally, the samples were washed 3 times with PBS, 5 min per time, developed by DAB, microscopically observed, and photographed. The primary antibodies for IL-1β (1:200, ab9722), Osx (1:1000, ab 22,552) and iNOS (1:100 ab49999) were purchased from Abcam (UK). The immunofluorescent staining sections for IL-1β and iNOS were blocked with 5% donkey serum for 30 min at room temperature, and then incubated with primary antibodies overnight at 4 °C. Alexa Fluor® 488-conjugated Donkey anti-rabbit IgG (1:200) and Alexa Fluor® 594-conjugated Donkey anti-mouse IgG (1:200) from Invitrogen (USA) were used as secondary antibodies. The cell nuclei were stained by DAPI (Sigma, USA) for 5 min at room temperature. The iNOS- and IL-1β-positive cells were investigated by a fluorescent microscope (Olympus Corporation, Japan) and analyzed with ImageJ software (National Institutes of Health, USA). The primary antibodies for IL-1β (1:200, ab9722) and iNOS (1:100 ab49999) were purchased from Abcam (UK).

2.10. Isolation and culture of bone marrow-derived MSCs

C57BL/6 mice were euthanized and soaked in 75% alcohol, and then dissected to obtain the long bones of their limbs. All muscles and cartilage tissues around the long bones were collected and washed in

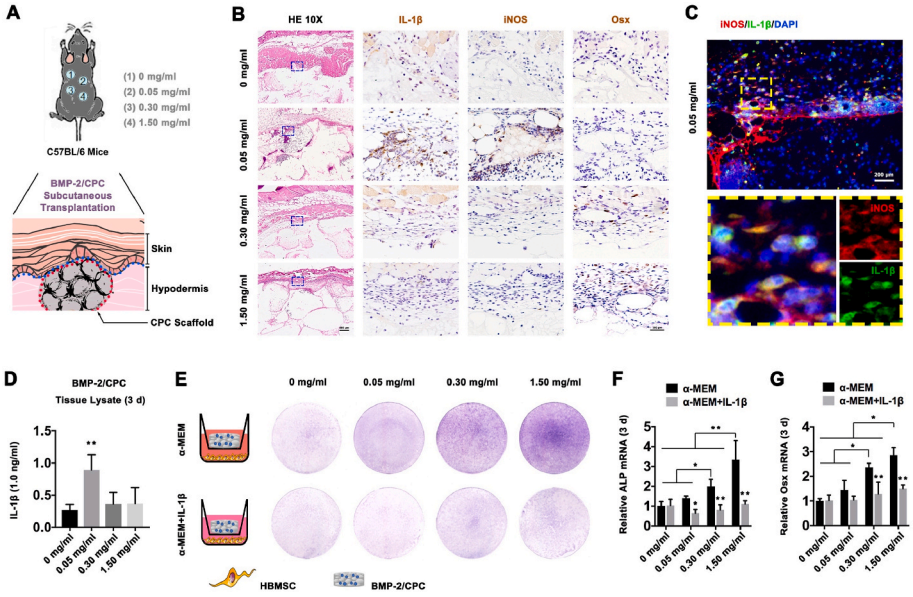

Fig. 2. IL-1β inhibited osteogenesis. [A] Schematic diagram of animal experiment. [B] In histological sections, expressions of IL-1β, iNOS (Marker of M1 phenotype macrophage), Osx (Osteogenic marker) were detected by immunohistochemistry in different doses of BMP-2 groups, Scale bar: 400 μm (HE staining) and 100 μm (immunofluorescent staining). [C] Co-localization of IL-1β and iNOS proteins in M1 macrophage were presented by immunofluorescence, Scale bar: 200 μm [D] IL-1β concentration in the tissue of BMP-2/CPC particles was detected by ELISA. [E] 1 ng/ml IL-1β was added to MSC-BMP-2/CPC co-culture system, MSC osteogenic differentiation was measured by alkaline phosphatase staining. [F, G] IL-1β inhibited MSCs' ALP mRNA expression and Osx mRNA expression.

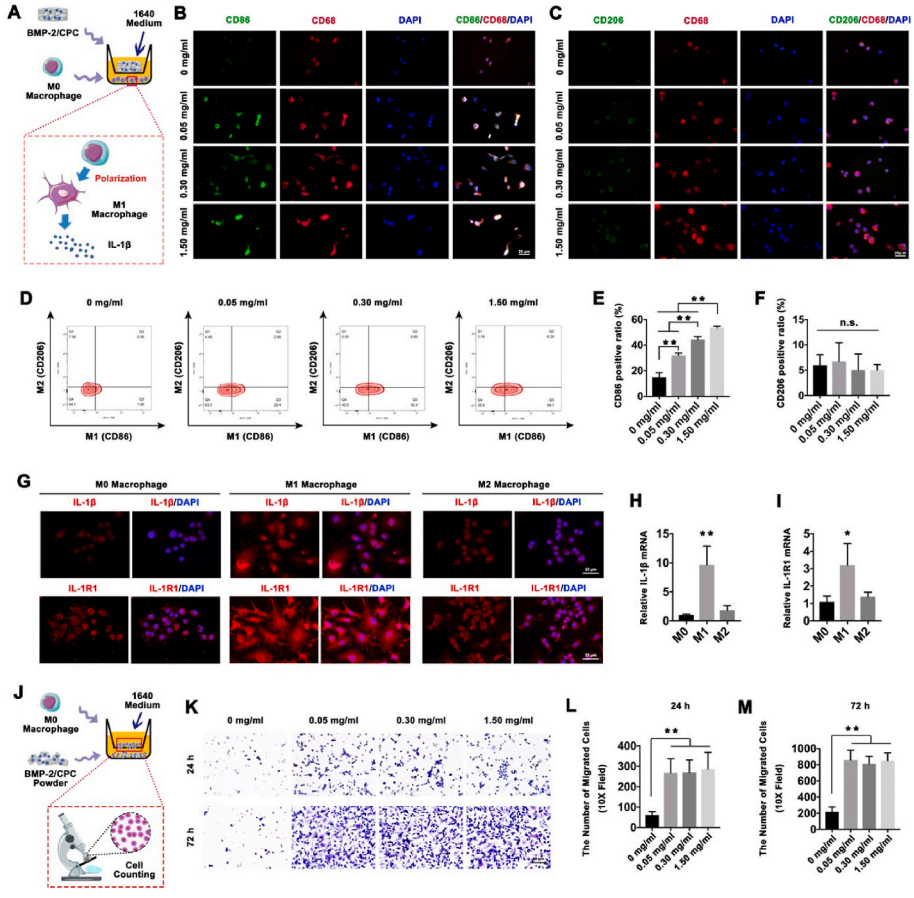

Fig. 3. BMP-2 induced M1 polarization, migration and IL-1β secretion. [A] Schematic diagram of the "macrophage-BMP-2/CPC" co-culture system for observing macrophage polarization induced by BMP-2. M0 macrophage was co-cultured with 0, 0.05, 0.3, 1.5 mg/ml BMP-2/CPC particles. [B] The expression levels of general macrophage marker (CD68) and M1 macrophage marker (CD86) were detected after a 3-d culture with M0 macrophages (Scale bar: 25 μm). [C] The expression levels of general macrophage marker (CD68) and M2 macrophage marker (CD206) were detected after a 3-d culture with M0 macrophages (Scale bar: 25 μm). [D] The proportions of macrophage subtypes in the four groups were investigated by flow cytometry. [E] Proportion of M1 (defined by CD86) at 3 d was analyzed. [F] Proportion of M2 (defined by CD206) at 3 d was analyzed. [G] The expressions of IL-1β and IL-1R1 in M0, M1 and M2 macrophages were presented by immunofluorescent staining (Scale bar: 25 μm). [H] The IL-1β mRNA expression in M0, M1 and M2 macrophages was detected by q-PCR. [I] The IL-1R1 mRNA expression in M0, M1 and M2 macrophages was detected by qPCR. [J] Schematic diagram of the "macrophage-BMP-2/CPC" co-culture system for observing macrophage migration induced by BMP-2. [K] At 24 h and 72 h, the images of migrated macrophages induced by BMP-2 were shown (Scale bar: 50 μm). [L] The migrated macrophages at 24 h were quantified and analyzed. [M] The migrated macrophages at 72 h were quantified and analyzed.

PBS. The epiphysis of each bone was cut off, and the bone marrow was flushed using a 27-gauge needle attached to a 10-ml syringe filled with PBS, to extract bone-marrow-derived MSCs. The MSCs from one mouse were collected by centrifugation, resuspended in α-MEM medium, and cultured for in *vitro* experiments. The MSCs were incubated at 37 °C, 5% CO_2. The medium was changed every 3 d.

2.11. Macrophage cell line culture

The macrophage cell line (RAW264.7) was purchased from Cobioer (Shanghai, China). The M0 macrophages were cultured in 1640 medium with 5% FBS at 37 °C, 5% CO_2. The M0 cells were induced into inflammatory M1 or anti-inflammatory and pro-regenerative M2 cells, according to previous protocols [26].

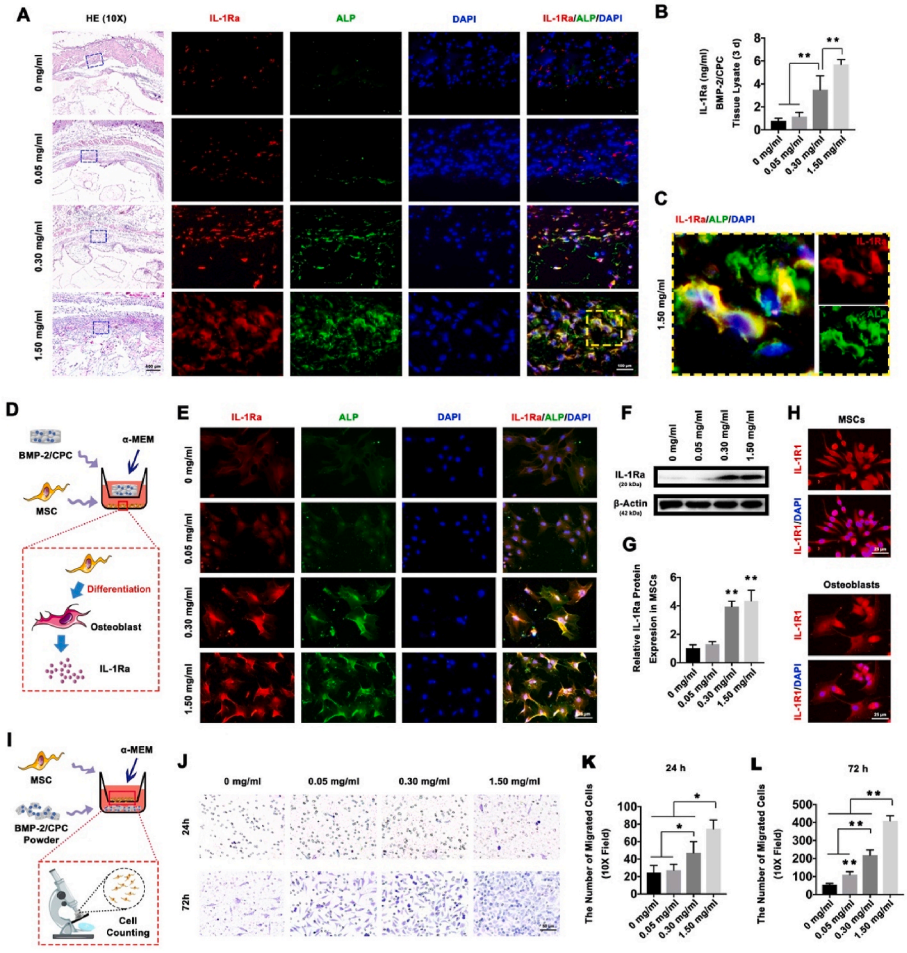

Fig. 4. BMP-2 induced MSC osteo-differentiation, migration and IL-1Ra expression. [A] With the increase of BMP-2 dose, IL-1Ra expression in ALP-positive cells was detected in the samples, Scale bar: 400 μm (HE staining) and 100 μm (immunofluorescent staining). [B] IL-1Ra concentrations in different groups of tissue lysates were examined by ELISA. [C] Co-localization of IL-1Ra and ALP proteins in osteoblasts were presented by immunofluorescence. [D] Schematic diagram of the "MSC-BMP-2/CPC" co-culture system for observing MSC osteo-differentiation induced by BMP-2. MSCs was co-cultured with 0, 0.05, 0.3, 1.5 mg/ml BMP-2/CPC particles. [E] IL-1Ra and ALP expression in BMP-2 treated MSCs were measured by immunofluorescent staining (Scale bar: 25 μm). [F] The IL-1Ra expression in BMP-2 treated MSCs was investigated by Western-Blot. [G] The relative IL-1Ra expression levels were analyzed by calculating the gray values. [H] The expression of IL-1R in MSCs and osteoblasts (Scale bar: 25 μm). [I] Schematic diagram of the "MSC-BMP-2/CPC" co-culture system for observing MSC migration induced by BMP-2. [J] At 24 h and 72 h, the images of migrated MSCs induced by BMP-2 were shown (Scale bar: 50 μm). [K] The migrated MSCs at 24 h were quantified and analyzed. [L] The migrated MSCs at 72 h were quantified and analyzed.

2.12. ALP activity analysis for IL-1β inhibited osteogenic differentiation in MSCs

MSCs (passage 3) were seeded in 24-well plates (25,000 cells per well) with 1 ml of α-MEM medium. When they adhered to the Transwell upper chambers (0.4-μm pore size) containing different doses of BMP-2/CPC particles, the MSCs and BMP-2/CPC particles were co-cultured with α-MEM medium or α-MEM medium containing murine IL-1β (1 ng/ml; PeproTech, USA). After 3 d, the medium and Transwell upper chambers were removed, and the lower chambers washed with PBS. The cells in the lower chambers were fixed with 4% polyformaldehyde at room temperature for 15 min, washed with water for 3 times, and stained with Alkaline Phosphatase Assay Kit (Beyotime, China) at 37 °C for 30 min. The staining was stopped by washing twice with running water. The stained cells were photographed.

2.13. Macrophage polarization induced by BMP-2/CPC particles

In the first day after operation, the M0 macrophages were seeded in 24-well plates (25,000 cells per well). After overnight culture, the four doses of BMP-2/CPC particles were placed in upper chamber of Transwell system, and co-cultured for 3 d with M0 macrophages from the second day. Then, the macrophages in the lower chambers were fixed with 4% polyformaldehyde at room temperature for 15 min, and washed with PBS for following immunofluorescent staining. The prepared samples were blocked with 5% donkey serum for 30 min at room temperature, and then incubated with primary antibodies overnight at 4 °C. Alexa Fluor® 488-conjugated Donkey anti-rabbit IgG (1:200) for iNOS, Donkey anti-goat IgG (1:200) for MMR and Alexa Fluor® 594-conjugated Donkey anti-mouse IgG (1:200) for CD68 were purchased from Invitrogen (USA). The cell nuclei were stained by DAPI (Sigma, USA) for 5 min at room temperature. The iNOS- and MMR-positive cells were investigated by a fluorescent microscope (Olympus Corporation, Japan) and analyzed with ImageJ software (National Institutes of Health, USA). The primary antibodies for CD68 (1:100, ab955), iNOS (1:100 ab15323) were purchased from Abcam (UK). The primary antibodies for MMR (1:100, AF2535) was purchased from R&D system (USA).

2.14. IL-1β and IL-1R1 expression in different macrophage subtypes

The M0 macrophages were polarized into M1 macrophages and M2 macrophages following previous reports [40]. The culture continued for 3 d. Then, the macrophages were fixed with 4% polyformaldehyde at room temperature for 15 min, and washed with PBS for following immunofluorescent staining. The prepared samples were blocked with 5% donkey serum for 30 min at room temperature, and then incubated with primary antibodies overnight at 4 °C. Alexa Fluor® 488-conjugated Donkey anti-rabbit IgG (1:200) for IL-1β or IL-1Ra. The primary antibodies for IL-1β (1:100, ab9722) and IL-1R1 (1:200, ab106278) were purchased from Abcam (UK).

2.15. Migration assay

For investigating BMP-2 recruitment effects on macrophages and MSCs, macrophages (RAW264.7) or MSCs (25,000 cells/chamber) were seeded in the Transwell upper chambers one night before migration assay, and cultured overnight. Next day, the BMP-2/CPC particles were

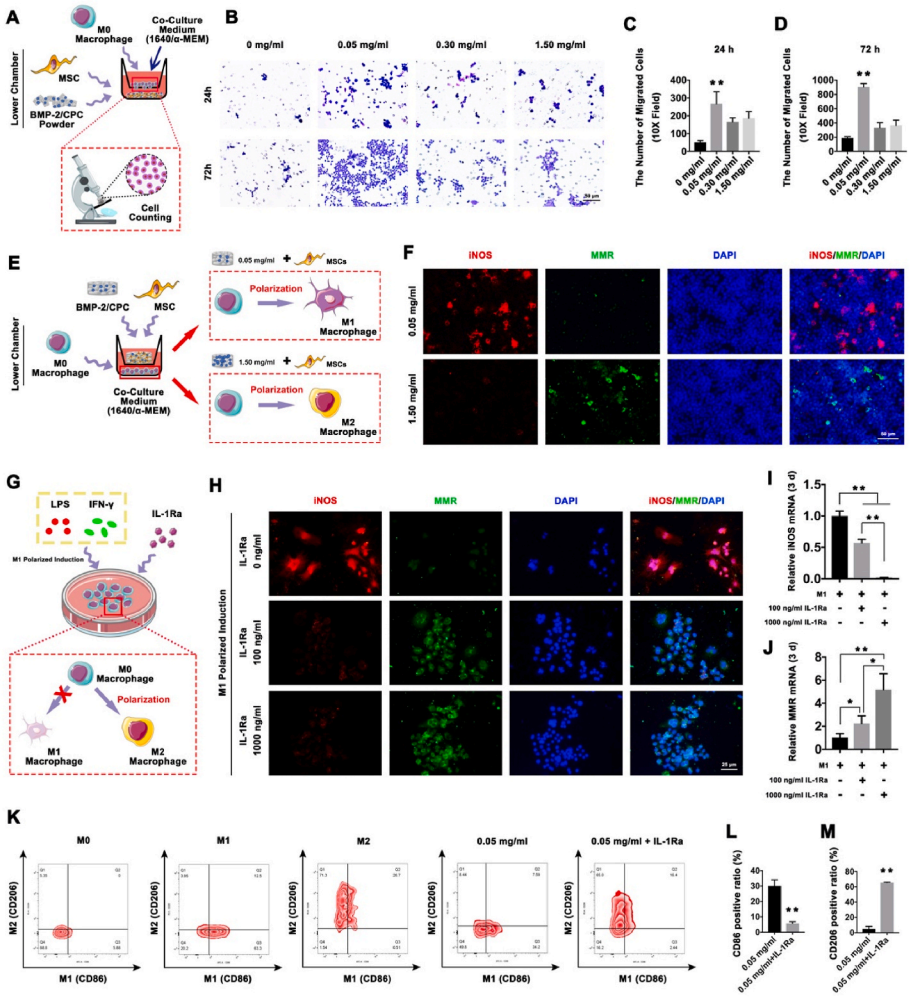

Fig. 5. Interaction between macrophages and MSCs. [A] Schematic diagram of the "macrophage-MSC-BMP-2/CPC" co-culture system for observing macrophage migration. [B] At 24 h and 72 h, the images of migrated macrophages were shown (Scale bar: 50 μm). [C] The migrated macrophages at 24 h were quantified and analyzed. [D] The migrated macrophages at 72 h were quantified and analyzed. [E] Schematic diagram of the "macrophage-MSC-BMP-2/CPC" co-culture system for observing macrophage polarization. [F] Macrophage subtype markers of M1 (iNOS) and M2 (MMR) macrophages were characterized after co-culturing for 3 d (Scale bar: 50 μm). [G] Schematic diagram of observing macrophage polarization induced by IL-1Ra. [H] Immunofluorescent staining was used to detect macrophage subtype markers of M1 (iNOS) and M2 (MMR) macrophages after IL-1Ra induction for 3 d (Scale bar: 25 μm). [I] The iNOS mRNA expression in M1 macrophages was detected by qPCR after IL-1Ra induction for 3 d. [J] The iNOS mRNA expression in M1 macrophages was detected by qPCR after IL-1Ra inducing for 3 d. [K] The proportions of macrophage subtypes in 0.05 mg/ml group and 0.05 mg/ml + IL-1Ra group were investigated by flow cytometry. The M0, M1 and M2 macrophages served as negative control, positive control respectively. [L] Proportion of M1 (defined by CD86) at 3 d was analyzed. [M] Proportion of M2 (defined by CD206) at 3 d was analyzed.

crushed and placed into Transwell bottom chambers. The Transwell upper chambers containing the cells were added onto the bottom chambers, and the culture medium was replaced with low-serum medium. The cells having migrated through the membrane was counted in three random fields.

For investigating the macrophage migration in co-culture system, MSCs (passage 3) were seeded in the bottom chambers containing BMP-2/CPC particles and cultured overnight. Macrophages (RAW264.7) were seeded in the Transwell upper chambers and also cultured overnight. Next day, the Transwell upper chambers were added onto the bottom chambers. The medium in the upper chambers was 1640 medium and the medium in the bottom chambers was α-MEM. The cells having migrated through the membrane were counted in three random fields.

2.16. M2 macrophage polarization induced by MSCs-released IL-1Ra

M0 macrophages were seeded in 24-well plates (25,000 cells/well) at the first day. At the same time, the MSCs (25,000 cells/chamber) were seeded in the upper Transwell chambers. The M0 macrophage and the MSCs were cultured separately overnight. Next day, 0.05 mg/ml and 1.50 mg/ml BMP-2/CPC particles were crushed and placed in upper Transwell chambers. The M0 macrophages, the MSCs and two doses of BMP-2/CPC particles were co-cultured for the following 3 d. Then, the macrophages in the lower chambers were fixed with 4% polyformaldehyde at room temperature for 15 min, and washed with PBS for following immunofluorescent staining. The prepared samples were blocked with 5% donkey serum for 30 min at room temperature, and then incubated with primary antibodies overnight at 4 °C. Alexa Fluor® 488-conjugated Donkey anti-rabbit IgG (1:200) for iNOS and Donkey anti-goat IgG (1:200) for MMR from Invitrogen (USA) were used as secondary antibodies. The cell nuclei were stained by DAPI (Sigma, USA) for 5 min at room temperature. The primary antibodies for iNOS (1:100 ab15323) were purchased from Abcam (UK). The primary antibodies for MMR (1:100, AF2535) were purchased from R&D system (USA).

2.17. Release of IL-1β and IL-1Ra in tissues around BMP-2/CPC particles

BMP-2/CPC particles at different doses were subcutaneously transplanted to C57BL/6 mice. Three days afterward, the particles and the surrounding tissues were collected. The 0 mg/ml BMP-2/CPC group served as a control. The tissue samples were incubated in 1 ml of tissue protein extraction reagent (Sigma-Aldrich, USA) containing protease inhibitors (1 tablet of protease inhibitor cocktail [Roche] for 10 ml) and homogenized with a tissue homogenizer. Tissue lysates were incubated for 1 h at 4 °C and centrifuged at 5000 g for 5 min. Cytokines were detected by ELISA (Mouse IL-1β and Mouse IL-1Ra, R&D Systems, USA) [31].

2.18. Flow cytometry for macrophage subtypes in BMP-2/CPC samples

2.18.1. For in vitro samples test

BMP-2/CPC particles at different doses were crushed and placed in upper Transwell chambers. The M0 macrophages were seeded in bottom

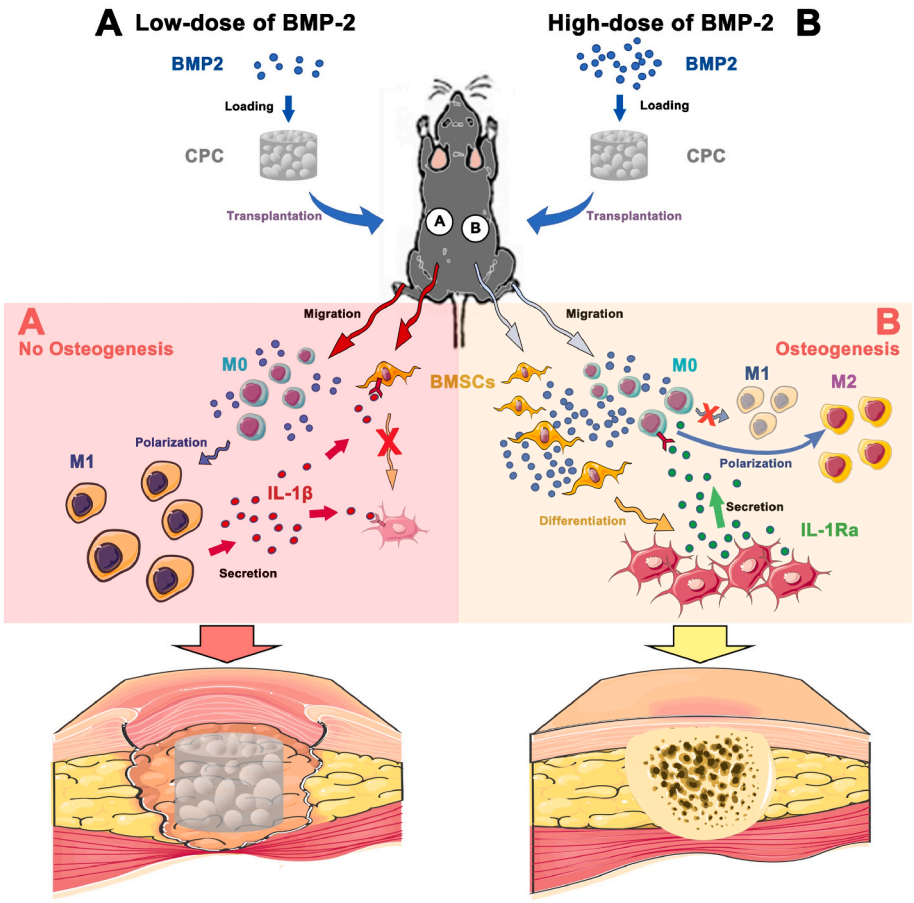

Fig. 6. Mechanisms of BMP-2-induced osteogenesis in a dose-dependent manner. At a low dose, BMP-2 recruited macrophages and polarized them into M1 subtype to release a large amount of IL-1β, which inhibits osteoblast differentiation and then limits bone regeneration. At a high dose, BMP-2 could also recruit macrophages, but more MSCs migrated and were induced into osteoblasts, which secrete mineralized matrix and release more IL-1Ra to promote M2-directing polarization, and then promote bone formation.

chamber and co-cultured with the BMP-2/CPC particles for the following 3 d. And then the upper chambers were discarded and fix the macrophages in bottom chamber with 4% polyformaldehyde at room temperature for 15 min, and washed with PBS for following incubating with mixture of antibodies (anti-CD86 APC and anti-CD206 PE, BioLegend, USA) for 30 min. The samples were tested on BD FACS Calibur (BD, USA). The data were analyzed with FlowJo software (TreeStar Inc., USA).

2.18.2. For in vivo samples test

BMP-2/CPC particles at different doses were subcutaneously transplanted to C57BL/6 mice. Three days afterward, the particles and surrounding tissues were collected. The 0 mg/ml BMP-2/CPC group served as a control. The harvested samples were mechanically broken down into smaller pieces and digested in Macrophage Isolation kit (Miltenyi Biotec, Germany); then, the digested samples were passed through 70-μm cell strainers and centrifuged. Cells were washed in PBS and labeled with LIVE/DEAD Zombie Aqua (1:500 dilution; BioLegend, USA) in PBS. Then, the cells were washed once with PBS, and incubated with the following antibodies from BioLegend (USA): anti-CD45 APC, *anti*-F4/80 PE, anti-CD11b FITC, anti-11c BV421, and anti-CD206 PE-Cy7. The samples were tested on BD FACS Calibur (BD, USA). The data were analyzed with FlowJo software (TreeStar Inc., USA).

2.19. Real-time polymerase chain reaction (qPCR)

RNA was extracted from the cells by using TRIzol reagent (Sigma, USA), and then transcribed into cDNA by the PrimeScript RT master mix (Takara, Japan). The genes of macrophage-markers and osteogenesis markers, including iNOS, MMR, IL-1β, IL-1R1, IL-1Ra, ALP and Osx, were assayed using a qPCR system (LightCycler® 480II; Roche, Switzerland). The relative gene expression levels were determined by the $2^{-\Delta\Delta Ct}$ method. The β-Actin was selected to normalize the expression levels of target genes. The results were presented as the fold change relative to that of the control group. All assays were carried out in triplicate.

Gene	Sequences of the primers
iNOS	F: TCACGCTTGGGTCTTGTTCA
	R: GGGGAGCCATTTTGGTGACT
MMR	F: CGCTCTAAGTGCCATCTCAGTTCA
	R: GACCTTCCATCTGCTCCACAATCC
IL-1β	F: ATGATGGCTTATTACAGTGGCAA
	R: GTCGGAGATTCGTAGCTGGA
IL-1R1	F: CCTGTGATTATGAGCCCACG
	R: CGTGTGCAGTCTCCAGAATATG
IL-1Ra	F: CGTGTGCAGTCTCCAGAATATG
	R: AAGAACACATTCCGAAAGTCAATAGG
ALP	F: ACCGCAGGATGTGAACTACT
	R: GAAGCTGTGGGTTCACTGGT
Osx	F: CGTCCTCTCTGCTTGAGGAA
	R: TTTCCCAGGGCTGTTGAGTC
β-Actin	F: GGCTGTATTCCCCTCCATCG
	R: CCAGTTGGTAACAATGCCATGT

2.20. Western-blot

The MSCs treated by different doses of BMP-2 were harvested, washed twice with cold PBS and lysed in RIPA lysis buffer (Beyotime, China) containing 1 mM phenylmethylsulphonyl fluoride (PMSF; Beyotime, China). The protein concentration was measured by Bradford protein assay. Protein (20 μg per lane) was loaded onto a 10% SDS-PAGE gel for electrophoresis, and then electroblotted (Bio-Rad, Hercules, CA, USA) onto 0.22 μm polyvinylidene fluoride (PVDF) membrane

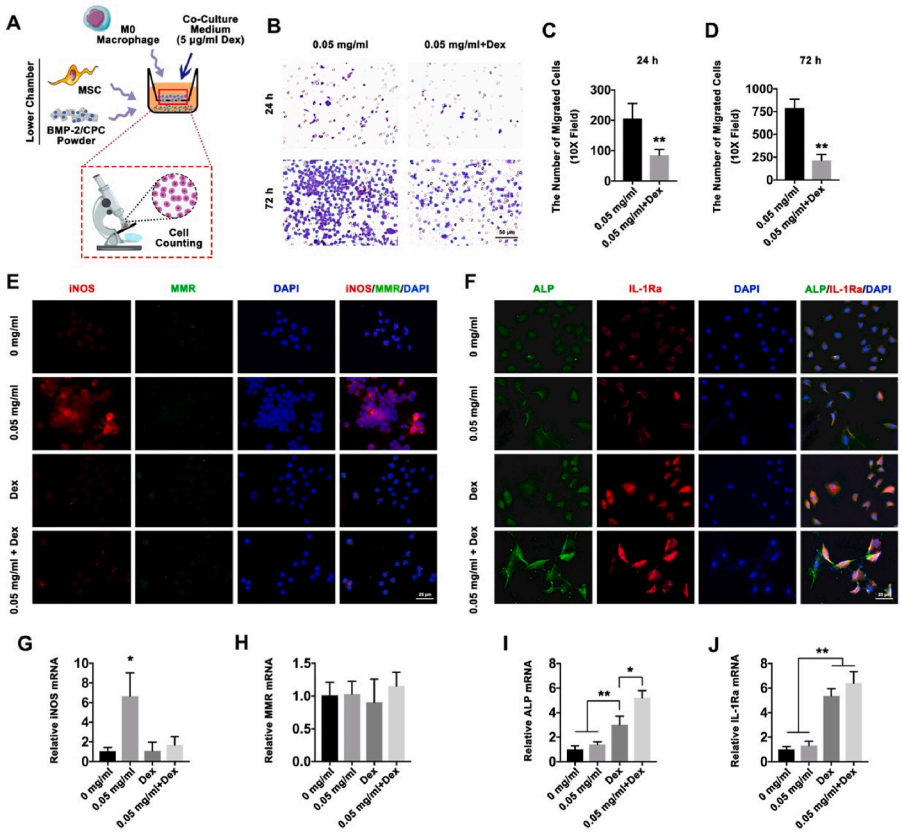

Fig. 7. Dex enhanced the osteogenic effect of 0.05 mg/ml BMP-2 *in vitro*. [A] Schematic diagram of the "macrophage-MSC-BMP-2/CPC" co-culture system for observing macrophage migration inhibited by Dex. [B] At 24 h and 72 h, the images of migrated macrophages were shown in the co-culture system with 5 μg/ml Dex (Scale bar: 50 μm). [C] The migrated macrophages at 24 h were quantified and analyzed. [D] The migrated macrophages at 72 h were quantified and analyzed. [E] Immunofluorescent staining was used to detect macrophage subtype markers of M1 (iNOS) and M2 (MMR) macrophages after co-culturing for 3 d with 5 μg/ml Dex (Scale bar: 25 μm). [F] Immunofluorescent staining was used to detect ALP expression and IL-1Ra expression in MSCs after co-culturing for 3 d with 5 μg/ml Dex (Scale bar: 25 μm). [G, H] iNOS and MMR mRNA expression levels in treated macrophages were measured by qPCR. [I, J] IL-1Ra and ALP mRNA expression levels in treated MSCs were measured by qPCR.

(Millipore, USA) at 300 mA for 1 h. PVDF membranes were blocked with blocking solution (5% skimmed milk) at room temperature for 1 h, and subsequently incubated with IL-1Ra (1:1000, ab124962) and β-Actin (1:1000, Bioworlde, Minneapolis, MN, USA) primary antibodies overnight at 4 °C. Finally, the membranes were washed with PBST (0.1% Tween-20 in 0.01 M PBS) incubated with secondary antibodies (1:2000, Boster, China) for 1 h at 37 °C, and then visualized with ImageQuant LAS4000 system (GE Healthcare, USA). β-Actin served as the control. The results were quantified with ImageJ software (National Institutes of Health, USA). The experiment was repeated for three times.

3. Results

3.1. Local osteogenesis and IL-1β activity at different doses of BMP-2

Previous clinical studies have found that 1.5 mg/ml BMP-2, an FDA-approved dose, can cause inflammatory side effects and excessive osteogenesis [4]. We evaluated the effect of this dose on tibial nonunion in mice. A model was constructed using mice with a femoral defect of 2 mm critical size [41]. Collagen sponges with different BMP-2 doses were applied to repair the femoral defects. Another bone formation model was established using mice subcutaneously implanted with BMP-2/CPC particles. As shown in Fig. 1B, micro-CT revealed that excessive bone tissues expanded beyond the femoral defect in 1.5 mg/ml group. The new bone volume of the four groups was significantly different by analyzing the data from micro-CT reconstruction (Fig. 1C). The similar excessive osteogenesis was observed around CPC particles in 1.5 mg/ml group (Fig. 1E and F). The significant differences were shown by analyzing the new bone distribution in the CPC particles (Fig. 1G and H). Fig. 1G illustrated the difference of total new bone area in the 0.30 mg/ml group and 1.5 mg/ml group, while Fig. 1H illustrated the difference of the new bone embedded in the scaffolds. New bone tissues also expanded in both 0.30 mg/ml groups of BMP-2/collagen sponges and BMP-2/CPC particles, but to an extent lower than that in 1.5 mg/ml groups. No osteogenesis was observed until the dose dropped to 0.05 mg/ml, one-thirtieth of FDA-approved BMP-2 dose. Other representative images within 14 d after treatment are shown in Supplementary Fig. 2. The similar osteogenic phenotypes were observed in the tissues around subcutaneously implanted silk sponges loaded with BMP-2 for 7 d *in vivo* (Supplementary Fig. 6A). According to a previous study [31], the osteogenic effect of BMP-2 was associated with IL-1β/IL-1R1 signaling. Thus, we further observed local IL-1β promoter activity after transplantation of BMP-2/CPC particles in C57BL/6-IL-1β$^{em1(Luc\text{-}eGFP)Smoc}$ mice. Unexpectedly, the fluorescence intensity did not increase with the dose of BMP-2. The data showed that the local IL-1β promoter activity in 0.05 mg/ml group exceeded those in the other three groups (Fig. 1J and K).

3.2. IL-1β inhibited osteogenesis

According to the results of IL-1β promoter activity in C57BL/6-IL-1β$^{em1(Luc\text{-}eGFP)Smoc}$ mice, we conducted ELISA and immunohistological staining to detect IL-1β expression around different BMP-2/CPC particles in the 3-d samples. The results showed a higher level of IL-1β in the 0.05 mg/ml group than in the other groups, with a local concentration of about 1 ng/ml. The immune cells expressing IL-1β were iNOS-positive M1 macrophages (Fig. 2B and C). In contrast, high levels of Osx-expressing osteoblasts were found in the 0.30 mg/ml group and 1.50 mg/ml group. *In vitro*, BMP-2/CPC particles induced MSCs to differentiate into osteoblasts. Osteogenic differentiation markers (Osx and ALP) of MSCs were up-regulated, with expression levels increasing with BMP-2 dose, but were inhibited by IL-1β (Fig. 2E–G). In 7-d *in vivo* samples of BMP-2/silk sponges, the expression trends of ALP and IL-1β were also obviously opposite (Supplementary Fig. 7A).

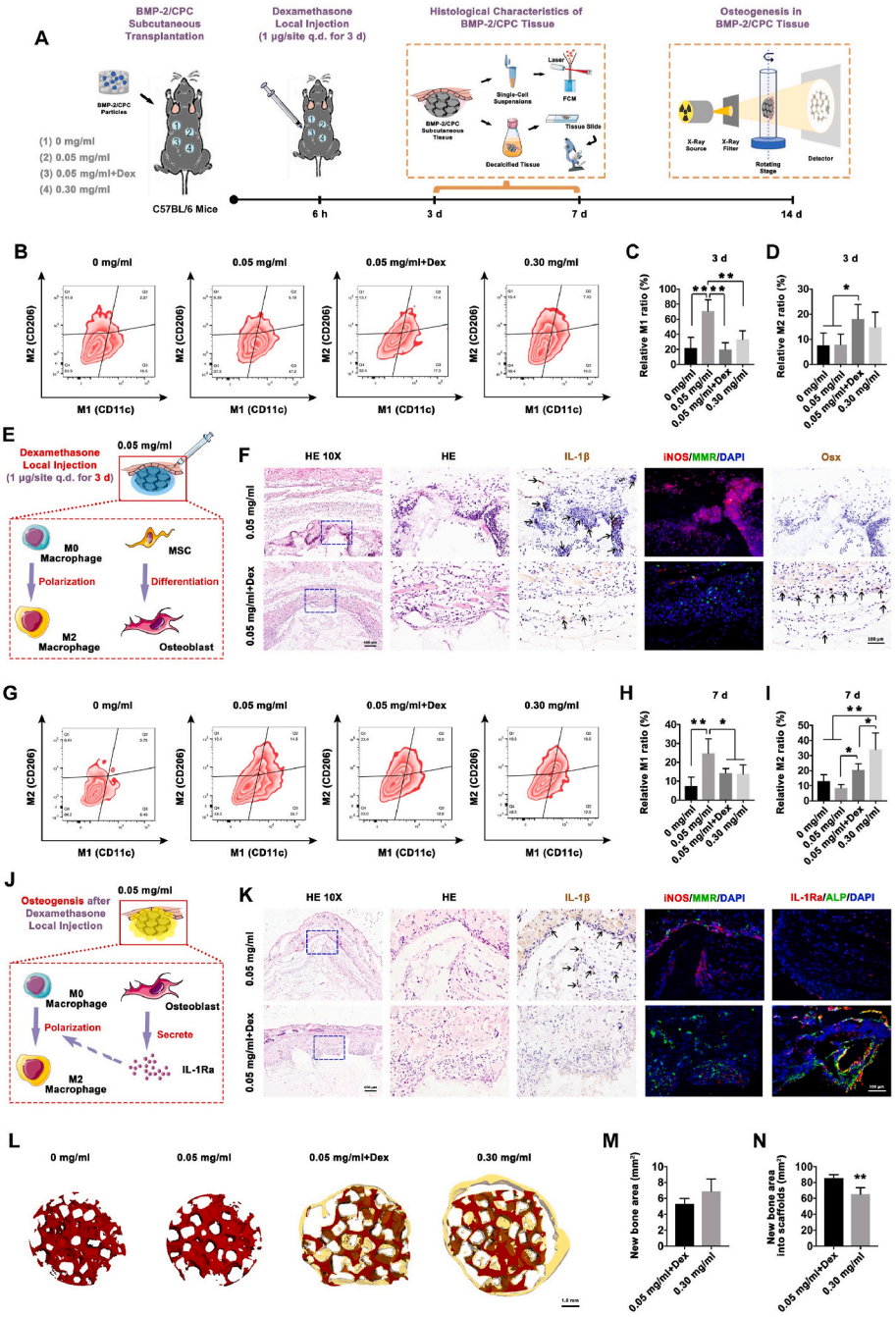

Fig. 8. Dex enhanced the osteogenic effect of 0.05 mg/ml BMP-2 *in vivo*. [A] Schematic diagram of Dex improved osteogenic effect of the 0.05 mg/ml group *in vivo*. Dex was injected once a day for 3 d from 6 h after operation. The partial samples were harvested at 3 d and 7 d to investigate the phenotypes of osteogenesis and macrophage infiltration in the tissue around transplanted BMP-2/CPC particles. The other samples were harvested at 14 d to investigate osteogenic effects by micro-CT. [B] The proportions of macrophage subtypes in the four BMP-2/CPC samples (3-d) were investigated by flow cytometry. [C] Proportion of M1 (defined by CD11c) in the BMP-2/CPC samples at 3 d was analyzed. [D] Proportion of M2 (defined by CD206) in the BMP-2/CPC samples at 3 d was analyzed. [E] Schematic diagram of Dex subcutaneous injection for 3 d to regulate MSC differentiation and macrophage polarization in local microenvironment. [F] The expressions of IL-1β, iNOS, MMR and Osx in the 3-d samples. [G] The proportions of macrophage subtypes in the four BMP-2/CPC samples (7-d) were investigated by flow cytometry. [H] Proportion of M1 (defined by CD11c) in the BMP-2/CPC samples at 7 d was analyzed. [I] Proportion of M2 (defined by CD206) in the BMP-2/CPC samples at 7 d analyzed. [J] Schematic diagram of osteogenesis after Dex local injection. Dex enhanced 0.05 mg/ml BMP-2/CPC particles to induce MSC osteogenic differentiation, secrete IL-1Ra and promote M2 polarization. [K] The expression levels of IL-1β, iNOS, MMR, IL-1Ra and ALP in the 7-d samples. [L] At 14 d, micro-CT showed new bone (marked as yellow) formed in the 0.05 mg/ml + Dex BMP-2/CPC group. Compared to the bone cyst formation in 0.30 mg/ml group, the new bone in 0.05 mg/ml + Dex BMP-2/CPC group was mainly distributed on the surface and in the pores of CPC particles. [M] The new bone area in the sections was analyzed by micro-CT. [N] The area of new bone growing into CPC particles in the sections was analyzed by micro-CT.

3.3. BMP-2 induced M1 polarization, migration and IL-1β secretion

Considering that IL-1β is mainly secreted by M1 macrophages, we investigated whether BMP-2 dose affects macrophage polarization. Without exception, different doses of BMP-2/CPC particles induced M0 into M1 macrophages and recruited the macrophages (Fig. 3B, C, D and K). We also detected the expression levels of IL-1β and IL-1R1 (key markers of IL-1/IL-1R1 signaling) in M0, M1 and M2 macrophages in order to analyze and illustrate how macrophages participated in the cross-talk with MSCs in following experiments. We also verified the expression levels of IL-1β and IL-1R1 in the macrophages induced from BMP-2 directly (Supplementary Fig. 4). Compared with M0 and M2, M1 expressed more IL-1β and IL-1R1 (Fig. 3G–I), suggesting that the osteogenesis in different BMP-2/CPC particles was not just related to the BMP-2 dose on macrophages (Fig. 3). Different osteogenic phenotypes should result from the interaction between macrophages and other factors in a bone-forming microenvironment.

3.4. BMP-2 induced MSC osteo-differentiation, migration and IL-1Ra expression

Given that all doses of BMP-2 could induce M1 polarization and enhance IL-1β release, we further investigated why only 0.05 mg/ml group exhibited M1 infiltration, IL-1β overexpression and low-scale new bone formation. In the other two groups treated with relatively high BMP-2 doses, some cells might promote osteogenesis under BMP-2 and release some cytokines to inhibit M1 infiltration. Thus, we suggested that MSCs might be significantly osteogenic at a certain dose of BMP-2, because they not only differentiate into osteoblasts, but also secrete IL-1Ra (a natural inhibitor of IL-1β). In the 3-d samples, IL-1Ra and ALP

were up-regulated by increasing BMP-2 dose *in vivo*, and ELISA results also showed that local IL-1Ra concentration increased with BMP-2 dose (Fig. 4A and B). *In vitro*, immunofluorescence staining and Western blotting determined that ALP positive cells could express IL-1Ra (Fig. 4D–F). Nevertheless, the number of migrated MSC increased significantly with BMP-2 dose (Fig. 4I–K). We confirmed that both MSCs and osteoblasts harbored IL-1R1 (Fig. 4H). As BMP-2/CPC particles did, different doses of BMP-2 silk sponges resulted in different profiles of osteogenesis and macrophage infiltration *in vivo* (Supplementary Fig. 7A).

3.5. Interaction between macrophages and MSCs

The above results confirmed that M1 macrophages, MSCs and osteoblasts expressed IL-1R1, while M1 macrophages expressed IL-1β and osteoblasts expressed IL-1Ra. We further skipped to whether the macrophages and MSCs interact under BMP-2 stimulation via secreting IL-1β and IL-1Ra. The number of migrated macrophages increased after adding MSCs to the co-culture system in 0.30 mg/ml and 1.50 mg/ml BMP-2/CPC groups (Fig. 5). Furthermore, M0 polarized towards M1 in 0.05 mg/ml group, but towards M2 in 1.50 mg/ml group (Fig. 5F). After the 3-d co-culture, the macrophages were further co-cultured for 5 d and fused into osteoclast precursors in 0.05 mg/ml group. The phenotypes were displayed by tartrate resistant acid phosphatase (TRAP) staining (Supplementary Fig. 8B). Whether is this difference related to the secretion of IL-1Ra? We polarized M0 towards M1 and added two doses of IL-1Ra simultaneously. Immunofluorescence staining and qPCR confirmed that IL-1Ra could promote M0 polarization towards M2, rather than M1 macrophages, even the M0 macrophages were cultured in the M1-inducing medium (Fig. 5G–J). When 1000 ng/ml IL-1Ra added to co-culture system of 0.05 mg/ml BMP-2 and M0 macrophages, the flow cytometry data showed M0 polarized towards M2 rather than M1 (Fig. 5K-M). The effect of IL-1Ra on other co-culture system of BMP-2/CPC and M0 macrophages was shown in Supplementary Fig. 9B flow cytometry data. We summarized how BMP-2 induced osteogenesis in a dose-dependent manner (Fig. 6).

3.6. Dexamethasone (Dex) enhanced the osteogenic effect of 0.05 mg/ml BMP-2 in vitro

We investigated whether we the osteogenic effect of 0.05 mg/ml BMP-2 can be enhanced by drugs that inhibit the M1 infiltration. Dex is an anti-inflammatory drug commonly used to suppress post-surgery inflammatory responses and tissue swelling [42,43]. In the present study, Dex (5 μg/ml) retarded the M1 polarization caused by BMP-2, while enhanced osteo-differentiation of MSCs (Fig. 7). Surprisingly, the expression of IL-1Ra in MSCs was significantly up-regulated by Dex in the medium (Fig. 7F). The migration of macrophages was also inhibited after Dex was added to the co-culture system composed of 0.05 mg/ml BMP-2/CPC particles, MSCs and macrophages.

3.7. Dex enhanced the osteogenic effect of 0.05 mg/ml BMP-2 in vivo

We then verified the therapeutic effects of Dex *in vivo*. We used 0 mg/ml BMP-2/CPC as negative control and 0.30 mg/ml BMP-2/CPC as positive control. BMP-2/CPC particles at different doses were subcutaneously transplanted into mice again, and Dex was injected locally once a day for first three days after operation. At 3 d, the samples of the four groups were collected and detected by flow cytometry. We found the M1/M2 ratios were opposite in 0.05 mg/ml group and 0.05 mg/ml + Dex group. The M1 infiltration and IL-1β expression in 0.05 mg/ml group (Fig. 8F) were as same as that in 0.05 mg/ml group (Fig. 2). When IL-1β neutralizing antibody was applied in 0.05 mg/ml group, we found obvious bone formation in this low dose group (as shown in Supplementary Fig. 11). However, the phenotypes were changed significantly by Dex. There was no obvious infiltrating M1 but Osx-positive cells in 0.05 mg/ml + Dex group (Fig. 8F). In the 7-d samples, the flow cytometry and immunohistological staining showed new bone tissues having developed in 0.05 mg/ml + Dex group (Fig. 8K). High levels of ALP and IL-1Ra positive cells and M2 macrophages (MMR positive macrophages) were observed in 0.05 mg/ml + Dex group (Fig. 8K). In 7-d BMP-2/silk sponges, Dex promoted osteogenesis in 0.05 mg/ml + Dex group (Supplementary Figs. 6B and 6B). At 14 d after transplantation, the samples were scanned with micro-CT and the images were reconstructed. No osteogenesis was observed in 0.05 mg/ml group, and new bone tissues were found in 0.30 mg/ml group. Compared with the excessive osteogenesis observed in 0.30 mg/ml group, the new bone tissues not only covered the surface of CPC particles but also filled some internal pores of CPC particles in 0.05 mg/ml + Dex group (Fig. 8L). Six micro-CT images of four groups are shown in Supplementary Fig. 10.

4. Discussion

In this study, we analyzed the relationships among inflammation, osteogenesis and BMP-2 dose. BMP-2 has been proven as a powerful growth factor in repairing bone defects [44]. Numerous studies focused on its effective doses [45,46], delivery routes [47,48] and functional fragment synthesis [49]. It remains unclear how BMP-2 induces immune responses which result in a series of complications such as fever, seroma, and local swelling in a fraction of patients [4]. Inflammatory infiltration in the fracture sites, if uncontrolled, may fail the healing and even lead to nonunion [50]. Our findings in this study may help design a therapeutic strategy that can overcome the limitations and enhance the osteogenic effects of BMP-2.

We verified the osteogenic effect of 1.5 mg/ml BMP-2 (an FDA-approved dosage) in two *in vivo* models. This dose induced osteogenesis around or even beyond the scaffolds. On the other hand, the osteogenesis was not observed in 0.05 mg/ml group. Interestingly, the immune response varied significantly across groups with different profiles of osteogenesis in C57BL/6-IL-1β$^{em1(Luc\text{-}eGFP)Smoc}$ mice. IL-1β is a critical proinflammatory cytokine. Previous studies have reported IL-1β can inhibit MSC proliferation and osteoblastic differentiation *in vitro* and interrupt bone healing *in vivo* [31]. Here we found that the high dose of BMP-2 repressed IL-1β expression via inhibiting M1 polarization and infiltration, while the low dose of BMP-2 enhanced IL-1β expression with increasing M1 macrophage infiltration.

However, our *in vitro* results confused us. We found all three doses of BMP-2/CPC particles induced M1 polarization and recruited macrophages, without significant differences (Fig. 3). Therefore, we hypothesized that two higher doses of BMP-2 might stimulate IL-1β expression and also activate other antagonistic factors to counteract the inflammatory effect of IL-1β in bone regeneration sites. After transplantation with BMP-2/CPC particles, multiple factors interact in various manners, thus leading to different local IL-1β expression levels. In tissues, the activity of cells is affected by exogenous factors, as well as endogenous factors via mechanism such as ligand-receptor binding [51,52]. We detected the expression of IL-1β and IL-1R1 in M0, M1 and M2 macrophage subtypes. IL-1R1 exists on the surface of almost all nucleated cells, and the expression of IL-1R1 differs with cell type [53]. Our results confirmed that M0, M1 and M2 macrophages expressed IL-1R1, but the IL-1R1 expression level in M1 macrophages was higher than those in the other two subtypes. The IL-1β, is mainly secreted by M1 macrophages, could act on themselves to further aggravate the inflammatory response.

We found that IL-1β expressions in both 0.30 mg/ml and 1.50 mg/ml groups were lower than that in 0.05 mg/ml group. One explanation may that a higher dose of BMP-2 can induce other cells in the bone-repairing microenvironment to release some cytokines capable of suppressing IL-1β or regulating macrophage polarization. One of these cytokines is IL-1Ra, a natural antagonist of IL-1β [54]. During MSCs osteo-differentiation, the released IL-1Ra can compete with IL-1β to bind to their shared receptor IL-1R1 [55]. IL-1Ra can not only restore the osteogenic ability of osteoblasts impaired by IL-1β [56], but also inhibit

macrophage M1 polarization [55]. Accordingly, we speculate that IL-1Ra plays a key role in promoting osteogenesis in 0.30 mg/ml and 1.50 mg/ml groups, as indicated by its higher *in vivo* expression in 0.30 mg/ml and 1.50 mg/ml groups than in control and 0.05 mg/ml groups. Co-cultured with 0.30 mg/ml and 1.50 mg/ml BMP-2/CPC particles, the MSCs-derived osteoblasts expressed ALP and IL-1Ra *in vitro*. The migration of macrophages was inhibited in 0.30 mg/ml group and 1.50 mg/ml group co-cultured with MSCs. However, the M1 polarization caused by BMP-2 was not achieved when MSCs were introduced to 1.50 mg/ml group. After two reported concentrations of IL-1Ra were added to M1-polarization-induction medium, the M0 macrophages that should be polarized towards M1 showed positive M2 markers (MMR) (Fig. 5). These *in vitro* results prove that upon higher dose of BMP-2, IL-1Ra secreted by osteoblasts could promote polarization towards M2.

We further clarified that BMP-2 regulates local macrophage-MSC interaction to promote osteogenesis. Dex, a common anti-inflammatory drug [57], has been used in osteogenic induction medium [58]. In the present study, we noticed that Dex could competitively inhibit M1 infiltration caused by 0.05 mg/ml BMP-2/CPC particles, and cooperate with BMP-2 products to induce osteogenic differentiation of MSCs and secretion of IL-1Ra. At a concentration previously reported [59,60], Dex changed M1/M2 ratio, IL-1β expression, percentage of ALP positive cells and IL-1Ra expression in the local sites. The therapeutic mechanism of this drug exactly matched the mechanism shown in Fig. 6 to optimize the osteogenic effect of BMP-2. It is worth noting that the application of Dex to optimize osteogenic effect of low-dose BMP-2 in this work was just an example. The effective dose of BMP-2 for clinical practice could be reduced by using some therapeutic strategies to regulate local macrophage function. We confirmed that other therapeutic strategies based on this mechanism could also achieve good osteogenic effects.

Subcutaneous implantation is a common and practical strategy in bone tissue engineering with a unique biologic entity that distinct from other areas of skeletal biology [61,62]. This strategy often was applied rodent models and have unique advantages over orthotopic (bone) environments, including a relative lack of bone cytokine stimulation and cell-to-cell interaction with endogenous (host) bone-forming cells [61]. This allows for relatively controlled *in vivo* experimental bone formation. We therefore selected the ectopic osteogenesis model to eliminate some complicated interfering factors. Most of our data were based on this relatively simple *in vivo* model. Further preclinical studies would be still needed to apply bone defect models to validate the effectiveness of our strategy on optimizing BMP-2 induced osteogenesis via regulating macrophage-MSC interaction.

5. Conclusion

In conclusion, the osteogenesis induced by BMP-2 was associated with interaction between macrophages and MSCs. BMP-2 at certain doses could induce MSCs differentiate into osteoblasts, and secrete IL-1Ra to inhibit M1 polarization and IL-1β release. The current FDA-approved BMP-2 dose could be optimized to improve osteogenesis from multiple perspectives, including bioactive materials, delivery mode, introduction of other anti-inflammatory drugs.

6. Statistical analysis

The data were expressed as means ± standard deviation (SD) and analyzed using one-way ANOVA and multiple *t* tests. *: $p < 0.05$, **: $p < 0.01$. The two-way ANOVA statistical analysis and multiple comparisons were performed to analyze the relative qPCR data of osteogenic markers in Fig. 2.

CRediT authorship contribution statement

Fei Jiang: contributed equally to this work, Conceptualization, Methodology, Software, Validation, Investigation, Writing – original draft. **Xuanyu Qi:** contributed equally to this work, Methodology, Software, Validation, Investigation. **Xiaolin Wu:** Methodology, Investigation. **Sihan Lin:** Methodology, Software, Investigation. **Junfeng Shi:** Formal analysis. **Wenjie Zhang:** Conceptualization. **Xinquan Jiang:** Conceptualization, Supervision, Project administration, Funding acquisition, Resources, Writing – review & editing.

Declaration of competing interest

The authors declare no conflict of interest.

Acknowledgments

This study was jointly supported by the National Natural Science Foundation of China (82130027, 81921002, 81900960, 82270955, 81991505), the Innovative Research Team of High-level Local Universities in Shanghai (SHSMU-ZLCX20212400) and the Project Funded by the Priority Academic Program Development of Jiangsu Higher Education Institutions (PAPD, 2018-87).

Appendix A. Supplementary data

Supplementary data to this article can be found online at https://doi.org/10.1016/j.bioactmat.2023.02.001.

References

[1] R.F. Heary, Anterior lumbar interbody fusion using rhBMP-2, J. Neurosurg. Spine 21 (6) (2014) 849–850.
[2] J.D. Conway, L. Shabtai, A. Bauernschub, S.C. Specht, BMP-7 versus BMP-2 for the treatment of long bone nonunion, Orthopedics 37 (12) (2014) e1049–e1057.
[3] P.H. Gomes-Ferreira, R. Okamoto, S. Ferreira, D. De Oliveira, G.A. Momesso, L. P. Faverani, Scientific evidence on the use of recombinant human bone morphogenetic protein-2 (rhBMP-2) in oral and maxillofacial surgery, Oral Maxillofac. Surg. 20 (3) (2016) 223–232.
[4] A.W. James, G. LaChaud, J. Shen, G. Asatrian, V. Nguyen, X. Zhang, K. Ting, C. Soo, A review of the clinical side effects of bone morphogenetic protein-2, tissue engineering, Part B, Reviews 22 (4) (2016) 284–297.
[5] M. Geiger, R.H. Li, W. Friess, Collagen sponges for bone regeneration with rhBMP-2, Adv. Drug Deliv. Rev. 55 (12) (2003) 1613–1629.
[6] T.H. Cho, I.S. Kim, B. Lee, S.N. Park, J.H. Ko, S.J. Hwang, (*) early and marked enhancement of new bone quality by alendronate-loaded collagen sponge combined with bone morphogenetic protein-2 at high dose: a long-term study in calvarial defects in a rat model, tissue engineering, Part. Accel. 23 (23–24) (2017) 1343–1360.
[7] B.B. Pradhan, H.W. Bae, E.G. Dawson, V.V. Patel, R.B. Delamarter, Graft resorption with the use of bone morphogenetic protein: lessons from anterior lumbar interbody fusion using femoral ring allografts and recombinant human bone morphogenetic protein-2, Spine (Phila Pa 1976 31 (10) (2006) E277–E284.
[8] Y.D. Wen, W.M. Jiang, H.L. Yang, J.H. Shi, Exploratory meta-analysis on dose-related efficacy and complications of rhBMP-2 in anterior cervical discectomy and fusion: 1,539,021 cases from 2003 to 2017 studies, J. Orthop. Translat. 24 (2020) 166–174.
[9] J. Vavken, A. Mameghani, P. Vavken, S. Schaeren, Complications and cancer rates in spine fusion with recombinant human bone morphogenetic protein-2 (rhBMP-2), Eur. Spine J. : official publication of the European Spine Society, the European Spinal Deformity Society, and the European Section of the Cervical Spine Research Society 25 (12) (2016) 3979–3989.
[10] M. Bannwarth, J.C. Kleiber, B. Marlier, C. Eap, J. Duntze, C.F. Litre, Ectopic bone formation with joint impingement after posterior lumbar fusion with rhBMP-2, Orthopaedics & traumatology, surgery & research : OTSR 102 (2) (2016) 255–256.
[11] R.D. Muchow, W.K. Hsu, P.A. Anderson, Histopathologic inflammatory response induced by recombinant bone morphogenetic protein-2 causing radiculopathy after transforaminal lumbar interbody fusion, Spine J. 10 (9) (2010) e1–e6.
[12] J.A. Rihn, J. Makda, J. Hong, R. Patel, A.S. Hilibrand, D.G. Anderson, A.R. Vaccaro, T.J. Albert, The use of RhBMP-2 in single-level transforaminal lumbar interbody fusion: a clinical and radiographic analysis, Eur. Spine J. : official publication of the European Spine Society, the European Spinal Deformity Society, and the European Section of the Cervical Spine Research Society 18 (11) (2009) 1629–1636.
[13] J.N. Zara, R.K. Siu, X. Zhang, J. Shen, R. Ngo, M. Lee, W. Li, M. Chiang, J. Chung, J. Kwak, B.M. Wu, K. Ting, C. Soo, High doses of bone morphogenetic protein 2 induce structurally abnormal bone and inflammation in vivo, Tissue engineering, Part. Accel. 17 (9–10) (2011) 1389–1399.

[14] Y. Chai, D. Lin, Y. Ma, Y. Yuan, C. Liu, RhBMP-2 loaded MBG/PEGylated poly (glycerol sebacate) composite scaffolds for rapid bone regeneration, J. Mater. Chem. B 5 (24) (2017) 4633–4647.

[15] R.M. de Freitas, C. Susin, W.M. Tamashiro, J.A. Chaves de Souza, C. Marcantonio, U.M. Wikesjö, L.A. Pereira, E. Marcantonio Jr., Histological analysis and gene expression profile following augmentation of the anterior maxilla using rhBMP-2/ACS versus autogenous bone graft, J. Clin. Periodontol. 43 (12) (2016) 1200–1207.

[16] Z. Schwartz, B.J. Simon, M.A. Duran, G. Barabino, R. Chaudhri, B.D. Boyan, Pulsed electromagnetic fields enhance BMP-2 dependent osteoblastic differentiation of human mesenchymal stem cells, J. Orthop. Res. 26 (9) (2008) 1250–1255.

[17] S.E. Kim, S.H. Song, Y.P. Yun, B.J. Choi, I.K. Kwon, M.S. Bae, H.J. Moon, Y. D. Kwon, The effect of immobilization of heparin and bone morphogenic protein-2 (BMP-2) to titanium surfaces on inflammation and osteoblast function, Biomaterials 32 (2) (2011) 366–373.

[18] J.H. Heo, J.H. Choi, I.R. Kim, B.S. Park, Y.D. Kim, Combined treatment with low-level laser and rhBMP-2 promotes differentiation and mineralization of osteoblastic cells under hypoxic stress, Tissue Eng Regen Med 15 (6) (2018) 793–801.

[19] S.J. Lee, D. Lee, T.R. Yoon, H.K. Kim, H.H. Jo, J.S. Park, J.H. Lee, W.D. Kim, I. K. Kwon, S.A. Park, Surface modification of 3D-printed porous scaffolds via mussel-inspired polydopamine and effective immobilization of rhBMP-2 to promote osteogenic differentiation for bone tissue engineering, Acta Biomater. 40 (2016) 182–191.

[20] M. Arifuzzaman, Y.R. Mobley, H.W. Choi, P. Bist, C.A. Salinas, Z.D. Brown, S. L. Chen, H.F. Staats, S.N. Abraham, MRGPR-mediated activation of local mast cells clears cutaneous bacterial infection and protects against reinfection, Sci. Adv. 5 (1) (2019), eaav0216.

[21] C. Zhong, X. Yang, Y. Feng, J. Yu, Trained immunity: an underlying driver of inflammatory atherosclerosis, Front. Immunol. 11 (2020) 284.

[22] A. Iwasaki, R. Medzhitov, Control of adaptive immunity by the innate immune system, Nat. Immunol. 16 (4) (2015) 343–353.

[23] R.S. Tarapore, J. Lim, C. Tian, S. Pacios, W. Xiao, D. Reid, H. Guan, M. Mattos, B. Yu, C.Y. Wang, D.T. Graves, NF-κB has a direct role in inhibiting bmp- and wnt-induced matrix protein expression, J. Bone Miner. Res. 31 (1) (2016) 52–64.

[24] L. Kong, Y. Wang, W. Smith, D. Hao, Macrophages in bone homeostasis, Curr. Stem Cell Res. Ther. 14 (6) (2019) 474–481.

[25] W.K. Hsu, M. Polavarapu, R. Riaz, A.C. Larson, J.J. Diegmueller, J.H. Ghodasra, E. L. Hsu, Characterizing the host response to rhBMP-2 in a rat spinal arthrodesis model, Spine (Phila Pa 1976 38 (12) (2013) E691–E698.

[26] D.M. Mosser, J.P. Edwards, Exploring the full spectrum of macrophage activation, Nat. Rev. Immunol. 8 (12) (2008) 958–969.

[27] N.C. Di Paolo, D.M. Shayakhmetov, Interleukin 1α and the inflammatory process, Nat. Immunol. 17 (8) (2016) 906–913.

[28] K. Wu, Y. Yuan, H. Yu, X. Dai, S. Wang, Z. Sun, F. Wang, H. Fei, Q. Lin, H. Jiang, T. Chen, The gut microbial metabolite trimethylamine N-oxide aggravates GVHD by inducing M1 macrophage polarization in mice, Blood 136 (4) (2020) 501–515.

[29] N.E. Powers, B. Swartzwelter, C. Marchetti, D.M. de Graaf, A. Lerchner, M. Schlapschy, R. Datar, U. Binder, C.K. Edwards 3rd, A. Skerra, C.A. Dinarello, PASylation of IL-1 receptor antagonist (IL-1Ra) retains IL-1 blockade and extends its duration in mouse urate crystal-induced peritonitis, J. Biol. Chem. 295 (3) (2020) 868–882.

[30] N. Parmar, P. Chandrakar, P. Vishwakarma, K. Singh, K. Mitra, S. Kar, Leishmania donovani exploits tollip, a multitasking protein, to impair TLR/IL-1R signaling for its survival in the host, J. Immunol. 201 (3) (2018) 957–970.

[31] Z. Julier, R. Karami, B. Nayer, Y.Z. Lu, A.J. Park, K. Maruyama, G.A. Kuhn, R. Müller, S. Akira, M.M. Martino, Enhancing the regenerative effectiveness of growth factors by local inhibition of interleukin-1 receptor signaling, Sci. Adv. 6 (24) (2020), eaba7602.

[32] H. Shen, J. Shi, Y. Zhi, X. Yang, Y. Yuan, J. Si, S.G.F. Shen, Improved BMP2-CPC-stimulated osteogenesis in vitro and in vivo via modulation of macrophage polarization, Mater Sci Eng C Mater Biol Appl 118 (2021), 111471.

[33] F. Wei, Y. Zhou, J. Wang, C. Liu, Y. Xiao, The immunomodulatory role of BMP-2 on macrophages to accelerate osteogenesis, tissue engineering, Part. Accel. 24 (7–8) (2018) 584–594.

[34] W. Zhang, L.S. Wray, J. Rnjak-Kovacina, L. Xu, D. Zou, S. Wang, M. Zhang, J. Dong, G. Li, D.L. Kaplan, X. Jiang, Vascularization of hollow channel-modified porous silk scaffolds with endothelial cells for tissue regeneration, Biomaterials 56 (2015) 68–77.

[35] M. Ishikawa, K.L. de Mesy Bentley, B.J. McEntire, B.S. Bal, E.M. Schwarz, C. Xie, Surface topography of silicon nitride affects antimicrobial and osseointegrative properties of tibial implants in a murine model, J. Biomed. Mater. Res., Part A 105 (12) (2017) 3413–3421.

[36] K.S. Kang, J. Lastfogel, L.L. Ackerman, A. Jea, A.G. Robling, S.S. Tholpady, Loss of mechanosensitive sclerostin may accelerate cranial bone growth and regeneration, J. Neurosurg. 129 (4) (2018) 1085–1091.

[37] J.Y. Kim, S.C. Kwak, S.J. Ahn, J.M. Baek, S.T. Jung, K.J. Yun, K.H. Yoon, J. Oh, M. S. Lee, Development of a novel frontal bone defect mouse model for evaluation of osteogenesis efficiency, J. Biomed. Mater. Res., Part A 103 (12) (2015) 3764–3771.

[38] K. Niwa, M. Nakamura, Y. Ohmiya, Stereoisomeric bio-inversion key to biosynthesis of firefly D-luciferin, FEBS Lett. 580 (22) (2006) 5283–5287.

[39] T. Hamada, K. Sutherland, M. Ishikawa, N. Miyamoto, S. Honma, H. Shirato, K. Honma, In vivo imaging of clock gene expression in multiple tissues of freely moving mice, Nat. Commun. 7 (2016), 11705.

[40] M. Orecchioni, Y. Ghosheh, A.B. Pramod, K. Ley, Macrophage polarization: different gene signatures in M1(LPS+) vs. Classically and M2(LPS-) vs. Alternatively activated macrophages, Front. Immunol. 10 (2019) 1084.

[41] B.H. Yoon, L. Esquivies, C. Ahn, P.C. Gray, S.K. Ye, W. Kwiatkowski, S. Choe, An activin A/BMP2 chimera, AB204, displays bone-healing properties superior to those of BMP2, J. Bone Miner. Res. 29 (9) (2014) 1950–1959.

[42] S.G.M. Falci, T.C. Lima, C.C. Martins, C. Santos, M.L.P. Pinheiro, Preemptive effect of dexamethasone in third-molar surgery: a meta-analysis, Anesth. Prog. 64 (3) (2017) 136–143.

[43] P.E. O'Hare, B.J. Wilson, M.G. Loga, A. Ariyawardana, Effect of submucosal dexamethasone injections in the prevention of postoperative pain, trismus, and oedema associated with mandibular third molar surgery: a systematic review and meta-analysis, Int. J. Oral Maxillofac. Surg. 48 (11) (2019) 1456–1469.

[44] V.S. Salazar, L.W. Gamer, V. Rosen, BMP signalling in skeletal development, disease and repair, Nat. Rev. Endocrinol. 12 (4) (2016) 203–221.

[45] J. Wang, Y. Zheng, J. Zhao, T. Liu, L. Gao, Z. Gu, G. Wu, Low-dose rhBMP2/7 heterodimer to reconstruct peri-implant bone defects: a micro-CT evaluation, J. Clin. Periodontol. 39 (1) (2012) 98–105.

[46] R.Y. Kim, J.H. Oh, B.S. Lee, Y.K. Seo, S.J. Hwang, I.S. Kim, The effect of dose on rhBMP-2 signaling, delivered via collagen sponge, on osteoclast activation and in vivo bone resorption, Biomaterials 35 (6) (2014) 1869–1881.

[47] D.B. Raina, I. Qayoom, D. Larsson, M.H. Zheng, A. Kumar, H. Isaksson, L. Lidgren, M. Tägil, Guided tissue engineering for healing of cancellous and cortical bone using a combination of biomaterial based scaffolding and local bone active molecule delivery, Biomaterials 188 (2019) 38–49.

[48] K. Stuckensen, J.M. Lamo-Espinosa, E. Muiños-López, P. Ripalda-Cemboráin, T. López-Martínez, E. Iglesias, G. Abizanda, I. Andreu, M. Flandes-Iparraguirre, J. Pons-Villanueva, R. Elizalde, J. Nickel, A. Ewald, U. Gbureck, F. Prósper, J. Groll, F. Granero-Moltó, Anisotropic cryostructured collagen scaffolds for efficient delivery of RhBMP-2 and enhanced bone regeneration, Materials 12 (19) (2019).

[49] M.A. Valdes, N.A. Thakur, S. Namdari, D.M. Ciombor, M. Palumbo, Recombinant bone morphogenic protein-2 in orthopaedic surgery: a review, Arch. Orthop. Trauma. Surg. 129 (12) (2009) 1651–1657.

[50] F. Loi, L.A. Córdova, J. Pajarinen, T.H. Lin, Z. Yao, S.B. Goodman, Inflammation, fracture and bone repair, Bone 86 (2016) 119–130.

[51] J. Nickel, T.D. Mueller, Specification of BMP signaling, Cells 8 (12) (2019).

[52] A.N. Combes, B. Phipson, K.T. Lawlor, A. Dorison, R. Patrick, L. Zappia, R. P. Harvey, A. Oshlack, M.H. Little, Single cell analysis of the developing mouse kidney provides deeper insight into marker gene expression and ligand-receptor crosstalk, Development 146 (12) (2019).

[53] D. Boraschi, P. Italiani, S. Weil, M.U. Martin, The family of the interleukin-1 receptors, Immunol. Rev. 281 (1) (2018) 197–232.

[54] J. Palomo, D. Dietrich, P. Martin, G. Palmer, C. Gabay, The interleukin (IL)-1 cytokine family–Balance between agonists and antagonists in inflammatory diseases, Cytokine 76 (1) (2015) 25–37.

[55] C.R. Harrell, B.S. Markovic, C. Fellabaum, N. Arsenijevic, V. Djonov, V. Volarevic, The role of Interleukin 1 receptor antagonist in mesenchymal stem cell-based tissue repair and regeneration, Biofactors 46 (2) (2020) 263–275.

[56] J. Petrasek, S. Bala, T. Csak, D. Lippai, K. Kodys, V. Menashy, M. Barrieau, S. Y. Min, E.A. Kurt-Jones, G. Szabo, IL-1 receptor antagonist ameliorates inflammasome-dependent alcoholic steatohepatitis in mice, J. Clin. Invest. 122 (10) (2012) 3476–3489.

[57] A. Lee, H.A. Blair, Dexamethasone intracanalicular insert: a review in treating post-surgical ocular pain and inflammation, Drugs 80 (11) (2020) 1101–1108.

[58] F. Langenbach, J. Handschel, Effects of dexamethasone, ascorbic acid and β-glycerophosphate on the osteogenic differentiation of stem cells in vitro, Stem Cell Res. Ther. 4 (5) (2013) 117.

[59] S. Zhang, J. Ermann, M.D. Succi, A. Zhou, M.J. Hamilton, B. Cao, J.R. Korzenik, J. N. Glickman, P.K. Vemula, L.H. Glimcher, G. Traverso, R. Langer, J.M. Karp, An inflammation-targeting hydrogel for local drug delivery in inflammatory bowel disease, Sci. Transl. Med. 7 (300) (2015), 300ra128.

[60] D. Bhargava, K. Sreekumar, A. Deshpande, Effects of intra-space injection of Twin mix versus intraoral-submucosal, intramuscular, intravenous and per-oral administration of dexamethasone on post-operative sequelae after mandibular impacted third molar surgery: a preliminary clinical comparative study, Oral Maxillofac. Surg. 18 (3) (2014) 293–296.

[61] M.A. Scott, B. Levi, A. Askarinam, A. Nguyen, T. Rackohn, K. Ting, C. Soo, A. W. James, Brief review of models of ectopic bone formation, Stem Cell. Dev. 21 (5) (2012) 655–667.

[62] M.R. de Misquita, R. Bentini, F. Goncalves, The performance of bone tissue engineering scaffolds in in vivo animal models: a systematic review, J. Biomater. Appl. 31 (5) (2016) 625–636.